

# Calliope $^{60}\text{Co}$ gamma irradiation facility for space qualification at ENEA-Casaccia research centre (Rome)

## Abstract

The radiation damage induced by hostile environment on optical and electronic components and devices underwent several studies since last decades. In order to evaluate the radiation damage on materials it is useful to irradiate them by energetic particles which simulate the radiation environment in which they will be used. The  $^{60}\text{Co}$  Calliope facility, located at the ENEA-Casaccia Research Centre (Rome), is involved in radiation processing researches and qualifications on materials and devices for hostile radiation environment, such as nuclear plants, Space and High Energy Physics experiments. This paper aims to highlight the importance of the qualification and research activities for Space applications and the key role of the Calliope gamma irradiation facility in this field. Some experimental results and researches performed on irradiated optical coating materials and commercial glassy substrates (BK7-B, BK7-G18 and Suprasil 2B) suitable for Space applications are discussed. While BK7-B shows a significant transmittance loss in the whole visible and ultraviolet range even at low gamma absorbed dose, BK7-G18 and Suprasil 2B appear to be good candidates for applications also in extreme environment.

**Keywords:** gamma radiation, irradiation facility, space qualification

Volume 3 Issue 2 - 2019

**S Baccaro, A Cemmi, I Di Sarcina**

ENEA – Fusion and Technology for Nuclear Safety and Security Department, Italy

**Correspondence:** Alessia Cemmi, ENEA – Fusion and Technology for Nuclear Safety and Security Department, Casaccia R. C., Via Anguillarese 301, S. Maria di Galeria, 00123 Rome, Italy, Tel +39 0630483169, Email [alessia.cemmi@enea.it](mailto:alessia.cemmi@enea.it)

**Received:** February 04, 2019 | **Published:** April 02, 2019

## Introduction

Optical and electronic components used on spacecrafts and satellites are exposed to a large variety of environments, often rich in high fluxes of energetic particles, which may cause serious degradation and damaging effects.<sup>1-5</sup> The Space experiment radiation environment is characterized by several kind of primary particles. The main sources of Space radiation are galactic cosmic rays, energetic electrons and protons, trapped in the Van Allen Belts, and particles associated to the solar activity (electron, protons and heavy ions). Cosmic rays are charged particles (protons, electrons and heavy ions) whose flux ( $10^{-28}$ - $10^3 \text{ m}^{-2} \text{ sr}^{-1} \text{ s}^{-1} \text{ GeV}^{-1}$ ) and particle energy (from tens to  $10^{14}$  MeV) vary depending on their solar, galactic and extra galactic origin.<sup>6-8</sup> The galactic cosmic rays flux strongly depends on the solar activity: it is low when the solar activity is high because the solar wind does not allow particles to easily enter the solar system. The charged particles of galactic cosmic rays are also influenced by the Earth magnetic field which provides a partial radiation shielding for spacecraft. However, cosmic rays, as well as solar emitted particles, have free access over the polar regions where the magnetic field lines are open to interplanetary Space: the result is that the galactic cosmic ray fluxes are higher at the Poles and lower at the equator.<sup>9</sup> The Van Allen belts mainly consist of MeV protons and keV electrons trapped in the Earth magnetic field, with a toroid spatial distribution around the Earth.<sup>10</sup> Trapped electrons are positioned in two regions: the former extends to about 2.4 Earth radii and contain electrons with energy lower than 5 MeV while the latter, the outer, goes from about 2.8 to 12 radii and include electrons with energy up to 7 MeV. Finally, the Sun is the source of different kinds of particles such as those produced by the solar wind coming from upper atmosphere of the Sun, and by the solar flares and the coronal mass ejection processes, sporadically occurring.<sup>9,11,12</sup>

The solar flares are enormous explosions in the solar atmosphere and cause the sudden bursts of Solar Energetic Particles (SEP), the heating of plasma to tens of millions of degrees and the eruption

of large amounts of solar mass.<sup>9</sup> SEP particles originated by solar phenomena are one of the dominant source of Total Ionization Dose (TID) effect in Space missions, as will be discussed in the following. Another source of radiation in Space is composed of the secondary particles (knock-out protons, neutrons,  $\alpha$ -particles, recoil nuclei and  $\gamma$ -rays) produced by the interaction of cosmic rays with spacecrafts and with the Earth atmosphere. In Low Earth Orbit (LEO), also albedo neutrons are sometimes mentioned, even if their component is small and of low energy. Secondary particles having energy exceeding  $10^{19}$  eV can initiate electromagnetic showers that are produced in a number of around 100 per year. Many showers die before arriving at the Earth surface, while the muons reach the sea level.<sup>13</sup> Moreover, typical radiation levels (in silicon) for Earth orbit missions are lower than 200 Gy with dose rate ranging from 1 to 100 Gy/y, while interplanetary missions experience higher absorbed dose (up to 10 kGy) and very low dose rate (magnitude of mGy/y).<sup>9,11,14,15</sup> The advent of particle physics and astrophysics experiments and, in general, the development of activities in Space, where detectors and components have to work in hostile radiation environment, has renewed the interest in the analysis of radiation-induced damage on electronic and optical devices. Astrophysics experiments, typically working at 300-600 km from the Earth surface, are exposed to energetic radiation as well as to a large variety of primary particles. For this reason, several radiation resistant materials are developed for use in Space instruments and setup.

In particular, specific interest is focused on the production and qualification of electronic devices that are very sensitive to radiation. In this sense, many researches aim to the optimization of commercial devices for application in hostile environment. The physical processes responsible of the radiation-induced damage on electronic devices are particularly complex. Depending on several parameters such as the radiation, its energy and its fluence and the electronic device type, it is possible to distinguish different damaging processes that may cause transient or cumulative effects. The first effect (Single Event

Effects SEE), can be induced by heavy particles (as neutrons) or high energy Compton electrons: these particles, instead of merely ionizing atoms or molecules, directly deposit their energy along their track, colliding with the lattice atoms and displacing them in interstitial positions. Total Non-Ionizing Dose (TNID) and TID are cumulative effects. TNID is induced by elastic or inelastic collision of particles with lattice atoms. The TID effect is induced by electrons,  $\gamma$ -rays and X-rays. The first step of this process consists of the transfer of radiation energy to the matter, as described in the following Section, which cause free hole-electron pairs production by ionization process. After their creation, hole-electron pairs may partially recombine or migrate through the material bulk under the influence of the electrical field. Finally, a fraction of them can be trapped in deep hole traps, inducing long term effects in the bulk with consequent alteration of the electrical characteristics of the electronic devices.<sup>11,16-21</sup>

Regarding the optical components for Space applications, a potential damage induced by radiation can be detrimental to the performances of the whole optical system. The typical radiation-induced effect consists of the transmittance loss due to the formation of charged defects (colour centres) and of network disorder increase. In particular, the interaction of gamma radiation with the optical materials is related to the creation of holes (HCs) and electrons (ECs) defects, able to absorb in the visible (VIS) and ultraviolet (UV) range, respectively.<sup>22,23</sup> In order to predict the radiation-induced damage on devices and components, it is useful to expose them to energetic particles fluxes, simulating the radiation environment in which they will operate. The ENEA  $^{60}\text{Co}$  Calliope facility presents specific and dedicated features extremely suitable for Space qualification activities and radiation damage researches on different kind of materials. The present paper aims to review the qualification and research activities on Space applications carried out at the Calliope facility in the last years. In addition a brief discussion of the main physical processes related to the radiation-matter interaction and the description of the Calliope facility are given. In the last section, some experimental results and researches performed on optical materials and components for Space applications are presented.

### Calliope gamma irradiation facility

The physical processes involved in the energy transfer mechanism from ionising radiation, such as X-rays and  $\gamma$ -rays, to matter depend on the energy of the impinging photons and on the kind of matter. Photoelectric, Compton, and pair-production represent the major absorption and attenuation processes for photons in the energy range from about 1 keV to 100 MeV and the relative importance of each process depends on the energy of the incident photons. In the energy region from 0.1 to 10 MeV, the Compton process dominates the total absorption. For materials with higher atomic number Z, the photoelectric process predominates at low energy values (up to 0.8

MeV), while pair production above around 5 MeV. In the region around 1 MeV, the Compton process is the most important, especially for low-Z materials, including all organics.<sup>24,25</sup> In order to study the gamma radiation-induced damage on devices and components, several activities are performed at the  $^{60}\text{Co}$  Calliope facility at ENEA Casaccia Research Centre (Rome, Italy).<sup>26</sup> Since the eighties, the facility has been involved in radiation processing research on agriculture, industrial materials (polymers and optical fibres) and on devices to be used in hostile radiation environment such as nuclear plants, Space experiments and High Energy Physics experiments. The Calliope facility is a pool-type irradiation facility equipped with a  $^{60}\text{Co}$   $\gamma$ -source in a high volume (7.0 m x 6.0 m x 3.9 m) shielded cell. The maximum licensed activity for the Calliope facility is  $3.70 \times 10^{15}$  Bq (100 kCi) and the present activity (January 2019) is  $2.59 \times 10^{15}$  Bq (70 kCi). Currently, source rack has a plane geometry with n. 25  $^{60}\text{Co}$  source rods (active area: 41 cm x 90 cm) (Figure 1A). The emitted  $^{60}\text{Co}$  radiation consists of photons of 1.17 and 1.33 MeV energy emitted in coincidence by the cobalt sources, with a mean energy of 1.25 MeV. At this energy value, the irradiated material is not activated and it can be safely manipulated immediately after the end of the irradiation. Moreover, due to the large dimensions of the irradiation cell, different dose rate values are available by placing the sample in specific positions during the irradiation tests. In particular, a steel platform, that covers the pool, allows the positioning of the samples close to the gamma source (maximum available dose rate: 10.80 kGy/h, January 2019). To obtain lower dose rate values, dedicated lead shielding can be used (together with a cubic (30 cm x 40 cm x 40 cm) and a cylindrical (24 cm diameter, 18 cm high) chambers with lead walls, allowing to achieve extremely low dose rates (lower than  $10^{-1}$  Gy/h) (Figure 1B). These positions are specific for the accommodation of different samples, such as electronics, biased and controlled using a feed through port during the irradiation tests. Two rotating platforms ensure a uniform absorbed dose distribution in case of high volume samples tests. Irradiation tests can be also performed in special environmental atmosphere (such as vacuum, gas mixtures other than air or different inert atmospheres) or at wide temperature range ( $-80^\circ\text{C} \div +80^\circ\text{C}$ ) and with a remote monitoring and acquisition. At the dosimetric laboratory of the Calliope facility different kinds of dosimetric systems are used: Fricke solution (20-200 Gy, periodically calibrated at Italian National Institute of Ionizing Radiation Metrology, INMRI), Red Perspex (5-50 kGy), TLD (0.1 mGy–100 Gy), ESR-alanine (up to about 500 kGy) and electronic RADFET (0.01–1000 Gy) dosimeters.<sup>24,27</sup> The facility is also equipped with diagnostic and single-camera systems. A dedicated irradiation process monitoring allows the issuing of irradiation certification to the customer. These certifications, stating the total absorbed dose, the irradiation time and the dose rate, are supported by dosimetric certification, in which the dose rate measurement performed in the specific position of the irradiated sample is reported.

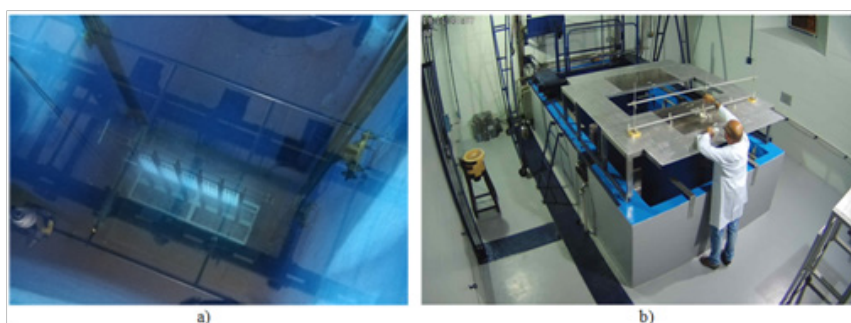


**Figure 1** A) Calliope rack with n. 25  $^{60}\text{Co}$  sources (pool view); B) irradiation cell view and movable supports for dosimetric measurements and cylindrical lead chamber for irradiation tests (left side).

## Research and qualification activities at Calliope $^{60}\text{Co}$ facility

In the last decades, the Calliope gamma irradiation facility has been deeply involved in research and industrial activities in the framework of national and international projects and collaborations with industries and research institutions.<sup>26</sup> A large part of activities are focused on the investigation of gamma irradiation effects on chemical and physical properties of different materials for several applications, such as radiation processing on industrial materials (polymers and optical fibres) and devices to be used in hostile radiation environment (nuclear plants, Space experiments and High Energy Physics experiments), scintillating materials (crystals and glasses) used as detectors in High and Medium Energy Physics experiments, ionizing damage evaluation tests on electronic components, Cultural Heritage, agriculture, AgroSpace and environmental applications.<sup>28-42</sup> Qualification tests are mainly performed on electronic components and devices for application in hostile environment such as nuclear plant and Space and on concrete matrices for nuclear waste disposal and storage.<sup>43,44</sup> At Calliope facility it is possible to perform ionizing damage test on electronic components according to MIL-STD-883E and/or ESCC BASIC SPECIFICATION No.22900 Issue 5 procedures.<sup>5,45-48</sup> Since 2018, The Calliope facility is indicated by the Italian Space Agency ASI as “ASI Supported Irradiation Facility” (ASIF Programme) recommended by the ESA, for carrying out the activities and the qualification tests for Space. The characterization analyses are carried out at the Calliope facility laboratory to investigate the gamma radiation effects induced in different materials. The laboratory is equipped with several instruments for the evaluation of optical (UV-VIS-NIR and Fourier Transform Infrared FTIR spectrophotometer, luminescence measurements), thermoluminescence and spectroscopic (Electron Spin Resonance ESR spectrometer) behaviour of materials after irradiation. The Calliope facility is also equipped with a climatic chamber for the ageing tests at different temperature (-75°C - +180°C) and relative humidity (10%-98%) of components under bias, controlled atmosphere and under UV light. A dedicated oven to perform the annealing of electronic devices after the irradiation tests together with furnaces for the thermal treatments of crystals and glasses are also available. An overview of some activities carried on at the Calliope facility related to gamma radiation effect on components and devices for Space applications are reported in the following sections.

### Qualification tests on electronic devices

The main effects associated to the interaction between gamma

radiation and electronic devices are a conductivity increase (because of the production of excess charged carriers) and charge trapping. In silicon, for example, the energy necessary to create a pair hole-electron is 3.6 eV and it is three times greater than silicon energy gap (1.1 eV). The interface damage defects are due to the presence of several trapping sites for charge carriers nearby the separation surface between Si and  $\text{SiO}_2$ . When ionizing radiation is absorbed by the oxide, several electron-holes pairs are generated and move under the electric field: electrons are quickly collected at the positive electrode, while holes go towards the Si-SiO<sub>2</sub> interface.<sup>11,18</sup> At Calliope gamma radiation facility it is possible to perform only TID damage qualification: for displacement damage tests ENEA neutrons facilities (TAPIRO and TRIGA-RC1 nuclear reactors and Frascati Neutron Generator-FNG) are available.<sup>49-51</sup> Electronic devices qualification tests performed at the Calliope facility are performed according to the special requirements specified in MIL-STD-883E and ESCC BASIC SPECIFICATION No.22900 Issue 5 procedures.<sup>5,45</sup> During the irradiation test, the specimens have to be surrounded by equilibrium material, which will minimize the dose enhancement from low energy scattered radiation by producing charge particle equilibrium: in this way, not photoelectric but only Compton effect occurs. To this purpose, both United States Military Standard (MIL) and ESA specifications recommend the use of a container of at least 1.5 mm of lead (Pb) with an inner lining of at least 0.7 mm of aluminium (Al). Considering the fraction of attenuated photons as a function of energy and thickness for Pb and Al (Figure 2), it is possible to establish that the 1.5 mm Pb (0.7 mm Al) layer absorbs 95% (99%) of the photons having energy lower than 150 keV (15 keV). The Pb or Al container approximately represents the charge particle equilibrium for silicon devices. According to the MIL specifications (standard conditions), the dose rate should be between 50 and 300 rads(Si)/s (1.8 and 10.8 kGy(Si)/h) and should not vary more than  $\pm 10\%$  during each irradiation. In accordance with the ESA specifications, two dose rate windows can be adopted: the standard dose rate from 3.6 krad to 36 krad/h (36 to 360 Gy/h) and the low dose rate from 36 to 360 rad/h (0.36 to 3.6 Gy/h). Depending on the expected maximum radiation level, the total exposition time should be less than 96 hours. Time interval between the end of exposition and the beginning of measurements of the device parameters should be less than 1 hour. Moreover, time interval between one completed exposition and the beginning of the next exposition should be at most 2 hours. At the end of irradiation tests, accelerated aging under bias can be also performed leaving the devices at room temperature for 24 hours and baking them at 100°C for 168 hours.

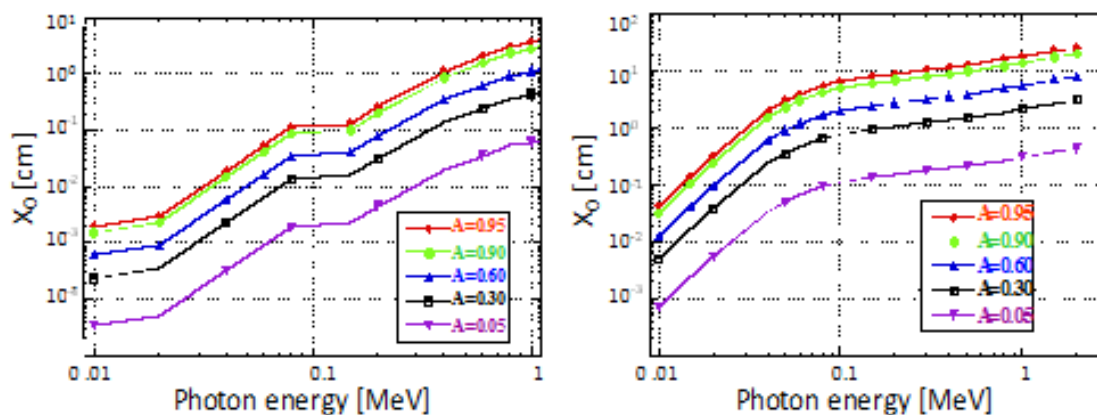
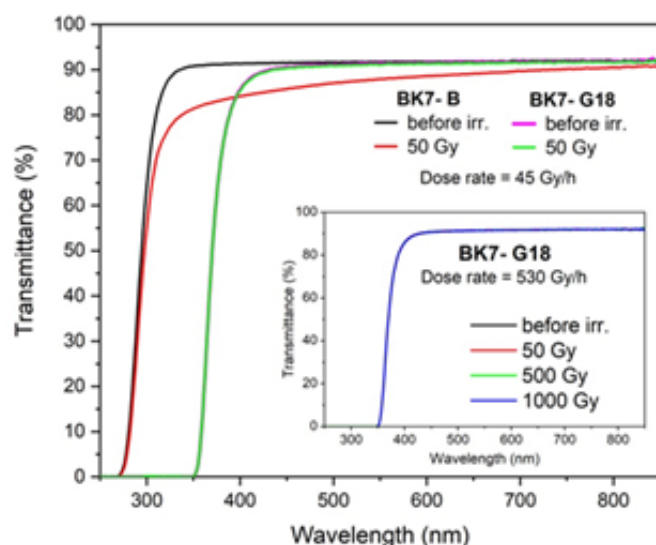
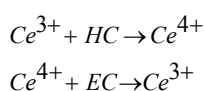


Figure 2 Lead (left) and aluminium (right) thickness as a function of the photon energy to obtain the attenuation at the percentage value reported in the inset.

## Characterization of optical components for space applications

In the last years, several researches were focused on the optical components (such as windows, lenses, optical mirrors, filters) operating in Space environment, since the exposition to fluxes of energetic particles may induce radiation damage and a consequent optical performances modification. Although specific qualification standards are not available for optical components, the characterization of their gamma radiation resistance represents an essential issue to be investigated prior to their use. For this reason, in order to simulate the hostile radiation environment, gamma irradiation tests were performed at the Calliope facility. Optical coatings and bulk substrates, used as lenses or windows, were investigated to study the radiation-induced optical damage in the UV-VIS-NIR spectral region. In this section, examples of the research activities performed at the Calliope facility on optical devices to be applied in Space are presented. Some researches performed in the past years, were focused on a set of optical coatings. The samples were submitted to gamma radiation with absorbed doses from 50 Gy (Low Dose Irradiation Test) up to 8.4 kGy (High Dose Irradiation Test) and 280 kGy (Very High Dose Irradiation Test). The analysed optical components, interesting for the UV-VIS-NIR spectral region, included single-layer coatings ( $\text{Al}_2\text{O}_3$ ,  $\text{Y}_2\text{O}_3$ , Mo, C, ZnO:Al, ITO), multi-layer coatings ( $\text{SiO}_2/\text{Ag}$ ) and Si bulk material.<sup>30,52,53</sup> The samples were prepared by Physical Vapor Deposition (PVD) on Suprasil 2B quartz substrate and reflectance and transmittance measurements were carried out by using a UV-VIS-NIR Perkin Elmer Lambda 900 Spectrophotometer. Our studies confirmed a stable behaviour of selected materials at 50 Gy absorbed dose. On the contrary, optical performances of samples irradiated at higher absorbed doses (8.4 kGy and 280 kGy) show significant deterioration in the investigated spectral region.<sup>53</sup>

Due to the influence of the substrates composition on the radiation hardness of the overall components, studies were also addressed to evaluate the behaviour of some of the most commonly used commercial glassy substrates. In particular, un-doped (BK7-B) and rad-hard Cerium-doped (BK7-G18, 1.8%wt of Cerium) multicomponent borosilicate glasses (produced by Schott) and high purity synthetic fused silica (Suprasil 2B produced by Heraeus) were compared to evaluate the effects of the absorbed dose and dose rate on these materials, used as substrates as well as optical windows. The total absorbed doses ( $\Delta D = \pm 3\%$ ) are calculated by using the dose rate value measured by Fricke solution dosimetry. Transmittance measurements were performed by UV-VIS-NIR Perkin Elmer Lambda 950 spectrophotometer ( $\Delta T = \pm 1\%$ ) and the thickness of the analysed glasses is 1 mm. The transmittance curves of BK7-B and BK7-G18 glasses before and after irradiation at 50 Gy absorbed dose and at the same dose rate (45  $\text{Gy}_{\text{air}}/\text{h}$ ) are reported in Figure 3. By comparing the curves before irradiation, the BK7-B shows high transparency in the VIS and UV range above around 270 nm, while the BK7-G18 presents an evident cut-off red-shift up to around 350 nm, due to the effect of cerium ions in the glass composition.<sup>54-56</sup> After irradiation, BK7-B transmittance loss in the whole UV-VIS range is caused by the formation of absorption bands of the radiation-induced holes (HC, VIS range) and of electrons (EC, UV range) defects, while no changes occur for the BK7-G18 rad-hard glass. This evidence can be explained by the competitive charge trapping mechanism of EC by  $\text{Ce}^{3+}$  and of HC by  $\text{Ce}^{4+}$  ions, as indicated in the following reactions:<sup>54</sup>



**Figure 3** Transmittance curves of BK7-B and BK7-G18 before and after irradiation at 50 Gy absorbed dose (dose rate= $45 \text{ Gy}_{\text{air}}/\text{h}$ ). Inset: Transmittance curves of BK7-G18 before and after irradiation at different absorbed doses (dose rate= $530 \text{ Gy}_{\text{air}}/\text{h}$ ).

The consequence of this process is the inhibition or the decrease of the radiation-induced colour centres, improving the radiation hardness of the cerium-stabilized glassy matrix. In the light of the results above discussed, the BK7-B glass does not appear to be a good material to be used in radiation environment because of its low radiation hardness. In order to study the absorbed dose and dose rate effects, studies were addressed to BK7-G18 rad-hard matrix. The experimental data reported in the inset in Figure 3 show no modification in term of transmittance values and cut-off position after irradiation at different absorbed doses up to 1000 Gy (dose rate= $530 \text{ Gy}_{\text{air}}/\text{h}$ ).

Similar results were obtained on BK7-G18 glass irradiated at low absorbed dose (50 Gy) and at two different dose rate values (45  $\text{Gy}_{\text{air}}/\text{h}$  and 530  $\text{Gy}_{\text{air}}/\text{h}$ ), as shown by the overlapping of the transmittance curves in Figure 4. The same sample was also irradiated at high absorbed dose (300 kGy) at dose rate of 530  $\text{Gy}_{\text{air}}/\text{h}$  and 2300  $\text{Gy}_{\text{air}}/\text{h}$ . In this case, the irradiation at the lowest dose rate value (45  $\text{Gy}_{\text{air}}/\text{h}$ ) was not performed due to the large irradiation time. Although no dose rate effect is still evident if the samples are irradiated at 300 kGy, the transmittance curves appear partially different if compared to that recorded before irradiation (Figure 4): a small transmittance reduction below around 500 nm and a cut-off red-shift of around 10 nm are observed. The BK7-G18 glass was also compared with Suprasil 2B quartz, a material of great interest for optical application due to its high transparency in the whole UV-VIS range. As shown in Figure 5, the transmittance curves of the samples irradiated at 1000 Gy absorbed dose present a very different trend below around 450 nm, with a BK7-G18 cut-off at 360 nm. Furthermore, Suprasil 2B was investigated under gamma irradiation up to 1000 Gy and no transmittance changes are shown (Figure 5). These results indicate that BK7-G18 glass as well as Suprasil 2B quartz can be considered for applications under irradiation in the VIS range, while only Suprasil 2B is suitable if high transmittance at shorter wavelengths is required.

Taking into account of the interesting features of Suprasil 2B quartz and in order to complete its characterization, irradiation tests under gamma and/or neutrons were performed at extreme conditions to test its behaviour in hostile environment. To this aim, Suprasil 2B samples were irradiated at very high gamma absorbed doses (1 MGy and 1.8 MGy) and at the TAPIRO fast neutron source reactor (total

neutron fluence =  $2.17 \times 10^{17}$  n/cm<sup>2</sup>); the additive effect of the highest gamma absorbed dose (1.8 MGy) followed by neutron irradiation was investigated on a third sample. The correspondent transmittance curves (Figure 6) show the formation of different absorption bands, associated to the creation of radiation-induced defects in silica matrix, after gamma and neutron irradiation. In particular, gamma irradiation is responsible of the absorption at around 210 nm, assigned to the dangling Si bonds (Si<sup>•</sup>), commonly indicated as generic E' centres,<sup>57</sup> and of the smaller absorption band at around 260 nm, associated to the dangling oxygen bonds ( $\equiv$ Si-O<sup>•</sup>), called "non-bridging oxygen hole centres" (or "NBOHCs").<sup>58</sup> An additional band at around 240 nm appears after neutrons irradiation and can be assigned to an "oxygen-deficiency centres" (or B<sub>2</sub> bands).<sup>59</sup> The increase of the E's and NBOHCs absorbance band intensities after neutron exposure is due to the gamma component always present in the TAPIRO mixed neutron-gamma field.

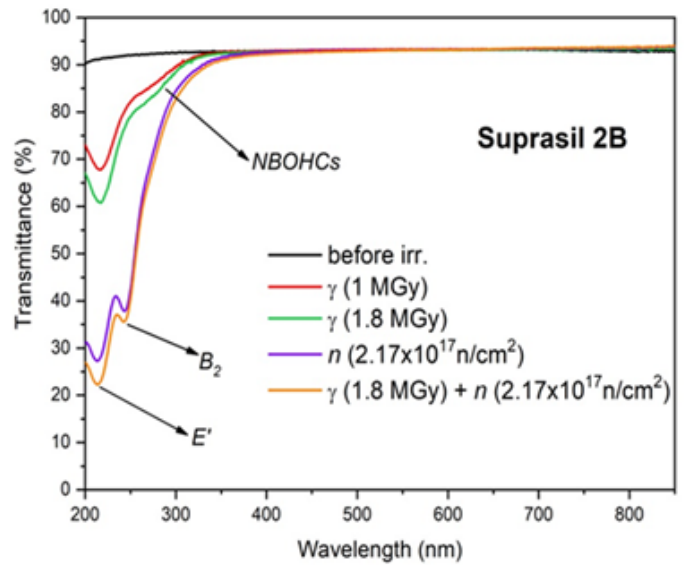


**Figure 6** Transmittance curves of Suprasil 2B before and after gamma irradiation at 1 MGy and at 1.8 MGy absorbed dose (dose rate=2300 Gy<sub>air</sub>/h), after neutron irradiation with total neutron fluence =  $2.17 \times 10^{17}$  n/cm<sup>2</sup> and after gamma irradiation at 1.8 MGy absorbed dose followed by neutron irradiation.

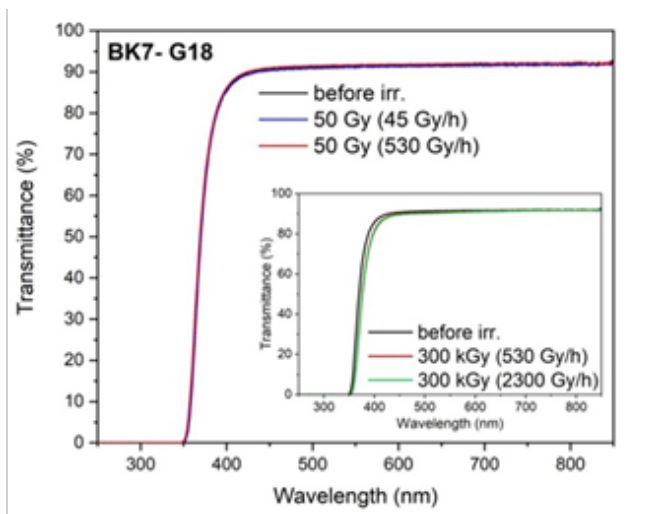


**Figure 4** Transmittance curves of BK7-G18 before and after 50 Gy absorbed dose and at different dose rates (45 Gy<sub>air</sub>/h and 530 Gy<sub>air</sub>/h). Inset: Transmittance curves of BK7-G18 before and after 300 kGy absorbed dose at different dose rates (530 Gy<sub>air</sub>/h and 2300 Gy<sub>air</sub>/h).

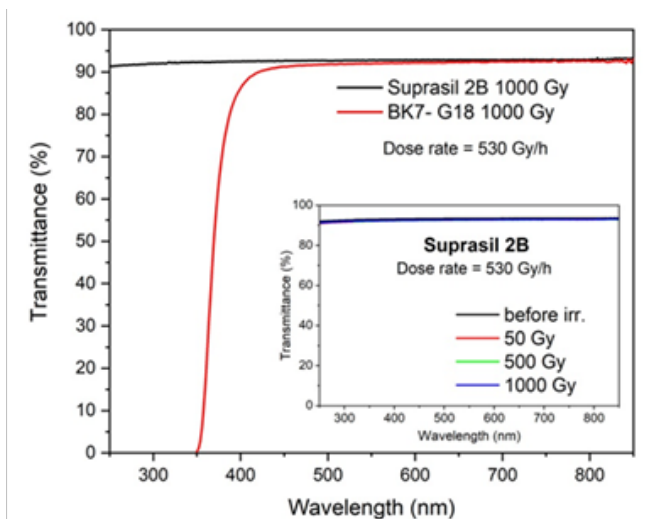


**Figure 5** Transmittance curves of Suprasil 2B and BK7-G18 after irradiation at 1000 Gy absorbed dose (dose rate=530 Gy<sub>air</sub>/h). Inset: Transmittance curves of Suprasil 2B before and after irradiation at different absorbed doses (dose rate=530 Gy<sub>air</sub>/h).

## Conclusion

In this paper, some issues concerning the application of electronic and optical components and devices in Space hostile environment are discussed. A description of the <sup>60</sup>Co Calliope irradiation facility (ENEA-Casaccia R.C., Rome, Italy) and electronic components qualification tests, performed according to MIL-STD-883E and/or ESCC BASIC SPECIFICATION No.22900 Issue 5 procedures, are given. Some example of research activities on optical components for Space applications are also presented. In particular, the experimental results on un-doped (BK7-B) and rad-hard Cerium-doped (BK7-G18) multicomponent borosilicate glasses and high purity synthetic fused silica (Suprasil 2B quartz), commonly used as substrates or optical windows, are discussed. BK7-G18 and Suprasil 2B show a good gamma radiation resistance and are stable in a wide absorbed dose range, independently on the dose rate values. BK7-G18 glass as well as Suprasil 2B quartz can be considered for applications under irradiation in the VIS range, while only Suprasil 2B is suitable if high transmittance in the UV range is required. The high purity Suprasil 2B silica presents good transparency above 350 nm also after very high gamma absorbed dose (up to 1.8 MGy) and neutron irradiation (total neutron fluence =  $2.17 \times 10^{17}$  n cm<sup>-2</sup>). In the UV range, the appearance of the gamma and neutrons radiation-induced defects absorption bands occurs.

## Funding details

The activities described in this work are partially funded by the Italian Space Agency (ASI) within the ASIF Supported Irradiation Facility Programme.

## Acknowledgments

Authors are very grateful to Mr. G. Ferrara for his precious and dedicated support during all the activities carried out at the Calliope facility and to Dr. F. Menchini for her contribution to the experimental measurements on glasses.

## Conflicts of interest

Authors declare that there is no conflict of interest.

## References

1. Binder D, Smith EC, Holman AB. Satellite anomalies from galactic cosmic rays. *IEEE Trans Nucl Sc.* 1975;22(6):2675–2680.
2. Albergo S, Azzi P, Babucci E. Test results of heavily irradiated Si detectors. *NIMA.* 1999;422(1-3):238–241.
3. Pickel JC, Blandford JT, Waskiewicz AE. Heavy ion induced permanent damage in MOS gate insulator. *IEEE Trans Nucl Sc.* 1985;32(6):4282–4286.
4. Waskiewicz AE, Groninger JW, Strahan VH, et al. Burnout of power MOS transistor with heavy ions of californium-252. *IEEE Trans Nucl Sc.* 1986;33:1710–1713.
5. *Total dose steady-state irradiation test method.* ESA/SCC Basic specification no. 22900 (Issue 5) European Space Agency. 2000.
6. Casadei D, Bindi V. The origin of cosmic ray electrons and positrons. *Astrophys J.* 2004;612(1):262–267.
7. Gordon MS, Goldhagen P, Peter Bailey. Measurement of the flux and energy spectrum of cosmic-ray induced neutrons on the ground. *IEEE Trans Nucl Sc.* 2004;51(6):3427–3434.
8. Nagano M, Watson AA. Observations and implications of the ultrahigh-energy cosmic rays. *Rev Mod Phys.* 2000;72(1):689–732.
9. Benton ER, Benton EV. Space radiation dosimetry in low Earth orbit and beyond. *Nucl Instrum Methods Phys Res B.* 2001;184(1-2):255–294.
10. Spurny F. Radiation doses at high altitudes and during space flights. *Radiat Phys Chem.* 2001;61:301–307.
11. Barth JL. *Space and Atmospheric Environments: from Low Earth Orbits to Deep Space.* In: Proceedings of Sixth Int. Space Conf. on Space Materials; 2003; NASA Goddard Space Flight Center, MD USA. 2003. Document ID: 20030053331.
12. Hafner JW. *Radiation shielding in space, Nuclear Science and Technology.* Academic Press, Inc; 1967.
13. BK Ridley. The Celestial sphere. In: John Wiley, et al., editors. *The Physical Environment.* Ellis Horwood Series in Environmental Science. Hoboken, USA. 1979:177–197.
14. Guo J, Zeitlin C, Wimmer-Schweingruber RF. Variations of dose rate observed by MSL/RAD in transit to Mars. *Astron Astrophys.* 2015;577A58:1–6.
15. Hassler DM, Zeitlin C, Wimmer-Schweingruber RF, et al. Mars' surface radiation environment measured with the Mars Science laboratory's Curiosity rover. *Science.* 2014;343(6169):1244797.
16. Brauning D, Wulf F. Atomic displacement and total ionizing dose damage in semiconductors. *Radiat Phys Chem.* 1994;43(1/2):105–127.
17. Gong H, Liao W, Zhang EX, et al. Proton-induced displacement damage and Total-Ionizing-Dose effects on silicon based MEMS resonators. *IEEE Trans Nucl Sc* 2018;65(1):34–38.
18. Messenger GC. *The effects of radiation on electronic system.* Van Nostrand Reinhold Company: New York; 1986.
19. Quinn H. Radiation effects in reconfigurable FPGAs. *Semicond Sci Technol.* 2017;32(4):1–8.
20. Sajid M, Chechenin NG, Sill Torres F, et al. Analysis of Total Ionizing Dose effects for highly scaled CMOS devices in Low Earth Orbit. *NIMB.* 2018;428(1):30–37.
21. Topper AD, Campola MJ, Chen D, et al. *Compendium of current total ionizing dose and displacement damage results from NASA goddard space flight center and NASA electronic parts and packaging program.* In: Proceedings of IEEE Radiation Effects Data Workshop (REDW); 2017 July 17-21; New Orleans, USA. Publisher city: USA; 2017. 8115431.
22. Baccaro S, Cecilia A, Cemmi A. Colour centres induced by  $\gamma$  irradiation in scintillating glassy matrices for middle and low energy physics experiments. *NIMB.* 2001;185(1-4):294–298.
23. Bishay A. Radiation induced color centers in multicomponent glasses. *J Non-Cryst Solids.* 1970;3(1):54–114.
24. Evans RD, *Radiation Dosimetry.* Attix FH, et al., editors. Vol. 1 Academic Press: New York; 1968.
25. Price WJ, *Nuclear Radiation Detection.* 2<sup>nd</sup> edn. New York: McGraw-Hill Book Co; 1964.
26. Baccaro S, Cemmi A, Di Sarcina I. Gamma irradiation Calliope facility at ENEA – Casaccia Research Centre (Rome, Italy). *Technical Report.* 2019;RT/2019/4/ENEA.
27. *ISO/ASTM 51026-15, Standard Practice for Using the Fricke Dosimetry System.* ASTM International, West Conshohocken, PA 2015.
28. Baccaro S, Cemmi A. Radiation activities and application of ionizing radiation on Cultural Heritage at ENEA Calliope gamma facility (Casaccia R.C., Rome, Italy). *Nukleonika.* 2017;62(4):261–267.
29. Baccaro S, Cemmi A, Cordelli M, et al. Radiation hardness test of undoped CsI crystals and Silicon Photomultipliers for the Mu2e calorimeter. *J Phys Conf Series.* 2017;928(1):012041.
30. Baccaro S, Piegari A, Di Sarcina I, et al. Effect of gamma Irradiation on Optical Components. *IEEE Trans Nucl Sc.* 2005;52(5):1779–1784.
31. Mihóková E, Nikl M, Pejchal J, et al. Luminescence and scintillation properties of  $\text{Y}_3\text{Al}_5\text{O}_{12}:\text{Pr}$  single crystal. *Phys Status Solidi C.* 2007;4(3):1012–1015.
32. Nikl M, Bohacek P, Mihóková E, et al. Radiation damage processes in wide-gap scintillating crystals. New scintillation materials. *Nucl Phys B-Proc Sup.* 1999;78:471–478.
33. Rossi P, Ferri de Collibus M, Florean M, et al. IVVS actuating system compatibility test to ITER gamma radiation conditions. *Fusion Eng Design.* 2013;88(9-10):2084–2087.
34. Chatrchyan S, Khachatryan V, Sirunyan AM, et al. Observation of a new boson at a mass of 125 GeV with the CMS experiment at the LHC. *Phys Lett B.* 2012;716(1):30–61.
35. Wang Y, Di Sarcina I, Cemmi A. Enhanced, shortened and tunable emission in  $\text{Eu}^{3+}$  doped borosilicate glasses by  $\text{Cu}^+$  co-doping. *Opt Mater.* 2019;87:80–83.
36. Pompili F, Esposito B, Marocco D. Radiation and thermal stress test on diamond detectors for the Radial Neutron Camera of ITER. *NIMA.* 2019.
37. Adams T, Adzic P, Ahuja S, et al. Beam test evaluation of electromagnetic calorimeter modules made from proton-damaged  $\text{PbWO}_4$  crystals. *J Instrum.* 2016;11(4)P04012.
38. Cova F, Moretti F, Fasoli M, et al. Radiation hardness of Ce-doped sol-gel silica fibers for High Energy Physics applications. *Optics Lett.* 2018;43(4):903–906.
39. Manoni E, Aloisio A, Baccaro S, et al. The upgrade of the Belle II forward calorimeter. *NIMA.* 2017;845:524–527.
40. Shen W, Baccaro S, Cemmi A, et al. Gamma-ray irradiation induced bulk photochromism in  $\text{WO}_3\text{-P}_2\text{O}_5$  glass. *NIMB.* 2015;362:34–37.

41. Massa S. *Anthocyanin bio-fortified colored tomato endowed with enhanced antioxidant capacity as a concept plant for space-based farming*. Conf. Proc. 3rd ISPMF (The International Society for Plant Molecular Farming) Congress 11-13/6/2018, Paasitorni Conference Center, Helsinki, Finland. 2001.
42. Corso AJ, Tassarolo E, Baccaro S, et al. Rad-hard properties of the optical glass adopted for the PLATO space telescope refractive components. *Optics Express*. 2018;26(26):33841–33855.
43. Dossier *Qualification of Nuclear Systems and Components – ENEA expertise and facilities*. Baccaro S, et al., editors. 2010.
44. IAEA Safety Standards Series No. GSG-1. "Classification of radioactive waste". 2009.
45. *Ionizing radiation (total dose) test procedure*, MIL-STD-883E, method 1019.4.
46. Abbate C, Alderighi M, Baccaro S, et al. Developments on DC/DC converters for the LHC experiment upgrades. *J Instrum*. 2014;9(2) C02017.
47. Ameer J, Amidei D, Baccaro S, et al. Radiation-hard power electronics for the ATLAS New Small Wheel. *J Instrum*. 2015;10(1)C01009.
48. Baccaro S, Bateman JE, Cavallari F. Radiation damage effect on avalanche photodiodes. *NIMA*. 1999;426(1):206–211.
49. Carta M, Burn KW, Console P. *TAPIRO fast spectrum research reactor characteristics for neutron radiation analyses*. In: European Nuclear Society. IGORR International Group on Research Reactors Proceedings; IGORR 18; 2018 Dec 3-7; Sidney, Australia. 2015.
50. Carta M, Falconi L, Fabrizio V. *A preliminary study for the utilization of the TRIGA RC-1 research reactor as a facility for radiation damage*. In: European Nuclear Society. RRFM European Research Reactor Conference Proceedings; RRFM 2016; 2016 13-17 March; Berlin, Germany. 2016.
51. Pietropaolo A, Andreoli F, Angelone M, et al. The Frascati Neutron Generator: A multipurpose facility for physics and engineering. *J Phys: Conf Ser*. 2018;1021(1):012004.
52. Di Sarcina I, Piegari A, Cecilia A. *Behavior of thin film materials under gamma irradiation for astronomical optics*. In: World Scientific Publishing. Astroparticle, Particle and Space Physics, Detectors and Medical Physics Applications; 9th Int. Conf. ICATPP; 2005 Oct 17-21; Villa Olmo, Como, Italy. Publisher's city: UK; 2006. p. 802.
53. Di Sarcina I, Ferrara G, Piegari A. *Thin-film optical materials under high dose gamma irradiation*. In: World Scientific Publishing. Astroparticle, Particle and Space Physics, Detectors and Medical Physics Applications; 10th Int. Conf. ICATPP; 2007 Oct 8-12; Villa Olmo, Como, Italy. Publisher's city: UK; 2008. p. 554.
54. Chen G, Du Y, Baccaro S. How cerium affects irradiation resistance. *American Ceramic Society Bulletin* 2001;80(4):107–110.
55. Baccaro S, Cecilia A, Mihokova E. Radiation damage induced by  $\gamma$  irradiation on  $\text{Ce}^{3+}$ -doped phosphate and silicate scintillating glasses. *NIMA*. 2002;476(3):785–789.
56. Baccaro S, Dall'Igna R, Fabeni P.  $\text{Ce}^{3+}$  or  $\text{Tb}^{3+}$ -doped phosphate and silicate scintillating glasses. *J Lumin*. 2000;87:673–675.
57. Griscom DL, Friebele EJ, Sigel GH. Observation and analysis of the primary  $^{29}\text{Si}$  hyperfine structure of the E' center in non-crystalline  $\text{SiO}_2$ . *Solid State Comm*. 1974;15(3):479–483.
58. Skuja L, Kajihara K, Hirano M, et al. Oxygen-excess-related point defects in glassy/amorphous  $\text{SiO}_2$  and related materials. *NIMB*. 2012;286:159–168.
59. Guzzi M, Martini M, Paleari A, et al. Neutron irradiation effects in amorphous  $\text{SiO}_2$ : optical absorption and electron paramagnetic resonance. *J Phys Condens Matter*. 1993;5(43):8105.